OPEN ACCESS

University of BRISTOL

Verderame, G., Ricci, P., De Luca, F., Del Gaudio, C., & De Risi, M. T. (2014). Damage scenarios for RC buildings during the 2012 Emilia (Italy) earthquake. *Soil Dynamics and Earthquake Engineering*, *66*, 385-400. https://doi.org/10.1016/j.soildyn.2014.06.034

Peer reviewed version

Link to published version (if available):
10.1016/j.soildyn.2014.06.034

Link to publication record in Explore Bristol Research
PDF-document

University of Bristol - Explore Bristol Research
General rights

This document is made available in accordance with publisher policies. Please cite only the published version using the reference above. Full terms of use are available:
http://www.bristol.ac.uk/red/research-policy/pure/user-guides/ebr-terms/

Damage scenarios for RC buildings during the 2012 Emilia (Italy) earthquake

Verderame Gerardo M., Ricci Paolo, De Luca Flavia,
Del Gaudio Carlo, De Risi Maria Teresa

University of Naples Federico II, DIST, Via Claudio 21, 80125 Napoli

Abstract

The main features of the Reinforced Concrete (RC) building stock that was struck by the Emilia 2012 earthquake and damage observed after the event are analyzed. Building stock characteristics and historical seismic classification are employed for the definition of two benchmark structures, representative of the whole building stock. Seismic capacity of the two structures, at different damage states, is assessed through static push-over analyses, within the N2 spectral assessment framework. Infill panels' contribution in terms of strength and stiffness is explicitly taken into account in the analytical model. Damage States are defined according to a mechanical interpretation of EMS-98 scale. Fragility functions at each Damage State are obtained through the application of a Response Surface Method. Finally large-scale damage scenarios are obtained crossing the geo-referenced census data regarding the characteristics of the Emilia RC building stock and starting from the seismic input provided by the shake map of the event. The scenarios seem to be in reasonable agreement with the observed damage.

Keywords*: Emilia earthquake, RC buildings, masonry infills, fragility curves, damage scenario, cumulative damage.*

1. INTRODUCTION

On the 20th of May 2012 a magnitude (M_w) 6.0 earthquake struck the Emilia region. The whole seismic sequence was characterized by seven events with M_w higher than 5.0. The area struck by the earthquake was very large; it included the provinces of Modena, Ferrara, Rovigo, and Mantova. Peak Ground Acceleration (PGA) registered at the closest station (epicentral distance equal to 16 km), during the mainshock, was equal to 0.27g (Chioccarelli et al., 2012). Most of observed damage involved masonry buildings, precast industrial structures, and, in some cases, Reinforced Concrete (RC) buildings, as shown by the photographic documentation collected after the event in different reconnaissance reports and papers (EPICentre Field Observation Report No. EPI-FO-200512, 2012; EPICentre Field Observation Report No. EPI-FO-290512, 2012; Parisi et al., 2012; Liberatore et al., 2013). The M_w 6.0 mainshock of the 20th of May was followed by another significant event of similar intensity (M_w=5.8, according to INGV) on the 29th of May.

A preliminary analysis of the performances of reinforced concrete (RC) buildings during the 2012 Emilia earthquake is provided herein. The general aim of the paper is to carry out a damage scenario analysis for the Emilia earthquake, thus providing a first, preliminary comparison with observed damage to RC buildings reported in reconnaissance reports.

During last years, several studies reported large scale post-earthquake comparisons between observed and predicted damage to the building stock in the areas struck by different seismic events (e.g., Spence et al., 2003; Kappos et al., 2007; Erberik, 2008; Tertulliani et al., 2011; Fiorini et al., 2012; Lin et al., 2012). Different seismic vulnerability assessment approaches were employed (observational, analytical or hybrid), and information on building stock characteristics was often provided by census data. Examples of preliminary loss assessment procedures were shown, too.

These studies allowed to show and discuss accuracy and reliability of applied damage estimation methodologies through a direct comparison between the results provided by the application of such methodologies and observational damage data.

In this study, damage scenarios are based on nonlinear static analyses on two benchmark structures, and fragility curves are obtained through a Response Surface Method. The two benchmark structures are representative of two classes of RC buildings composing the whole building stock. The analysis of building stock data and the study of the evolution of the seismic classification of the area highlight that most of the structures are low-medium rise buildings designed for gravity loads only, as shown in Sections 2 and 3. Section 4 describes main characteristics of the seismic sequence and observed damage to RC structures in the epicentral area.

According to the information collected on building stock and seismic classification, in Section 5 the two benchmark structures (2- and 4-storey high) have been defined as representative of the classes of RC buildings with less than four storeys and with four or more storeys, respectively. Infills structural contribution in terms of strength and stiffness has been taken into account. Seismic capacity of the two structures in terms of spectral acceleration and PGA, at different Damage States, is assessed through static push-over analyses, within the N2 spectral assessment framework, through an appropriate strength reduction factor - ductility - period (R-μ-T) relationship (Dolšek and Fajfar, 2004). The definition of Damage State thresholds in terms of displacement is made on a mechanical basis and through engineering judgment interpretation of the qualitative description provided by EMS-98 (Grünthal, 1998) (see Section 5).

In Section 6, vulnerability functions have been derived for the two structures representative of the two building classes at the defined Damage States, through the application of a Response Surface Method. Shake map data of the mainshock event occurred on the 20th of May 2012, according to INGV, and census data in terms of number of storeys and structural typology of the buildings (ISTAT, 2001) have been employed for the evaluation of damage scenarios for the municipalities struck by the event, and located in the epicentral area. The obtained damage scenarios is then compared with observed damage and photographic documentation collected right after the earthquake. The results of the vulnerability study and the observed damage allow a qualitative comparison given the fact that data of the official usability and damage inspections are not yet available. On the other hand, a fair agreement between observation and vulnerability functions can still represents a way to check the reliability of the adopted vulnerability approach, developed on a mechanical basis. Given the occurrence of the significant event of the 29th of May, a preliminary evaluation of cumulative damage on the two benchmark structures, resulting from the two main events (20th and 29th of May), is carried out.

2. MAIN FEATURES OF EMILIA BUILDING STOCK

The first step towards a vulnerability analysis is the identification of the main characteristics of the building stock in the considered area. The ISTAT (Italian National Institute of Statistics, *Istituto Nazionale di Statistica*) survey is a nation-wide census that provides information on citizens and buildings. In particular, in the 14th general census of population and dwellings (*14° Censimento generale della popolazione e delle abitazioni*) (ISTAT, 2001), information about characteristics of buildings are provided. The collected information concerns category of use (industrial or residential), structural typology (masonry, RC, …), number of storeys, and age of construction.

In the following, the above mentioned data are illustrated, referring to the area struck by the May 2012 Emilia seismic sequence. It is worth to note that age of construction needs to be accompanied by information regarding the evolution of the seismic classification, in order to identify the more common design approach characterizing the building stock of the area (see Section 3).

The availability of ISTAT data allows to evaluate the statistics of buildings in terms of number of storeys (1-, 2-, 3-, and ≥4-storey buildings), age of construction (typically with a decennial-rate),

and structural typology (masonry or RC buildings) for the spatial units of the census, the *census tracts*. Nevertheless, due to privacy requirements, these statistics are provided in aggregate format. Thus, for example, it is not possible to get the number of RC buildings in a census tract dating back to a specific age of construction and characterized by a given number of storeys. The statistics for the 448 Municipalities hit by the 2012 earthquake are shown in Figure 1.

Almost 5% of the whole building stock in the Emilia region is constituted by buildings or groups of buildings used for commerce, industry, communications or transport (Figure 1(a)). Within the area struck by the earthquake only 15% of buildings are RC structures (Figure 1(b)), and almost 75% of the buildings is one- or two-storey high (Figure 1(c)). A quite uniform distribution of the age of construction can be observed from data shown in Figure 1(d).

The information on the RC building stock gathered from ISTAT data can be compared with the corresponding information collected for L'Aquila (Abruzzo) area after the 2009 earthquake (e.g., Ricci et al., 2011). The comparison between Emilia and Abruzzo building stock data highlights a similar percentage of RC buildings (approximately equal to 20%) and similar distribution of number of storeys and age of construction. On the other hand, given the different evolution of the seismic classification, similar building stock characteristics can lead to different design approaches and, in turn, to different structural performances.

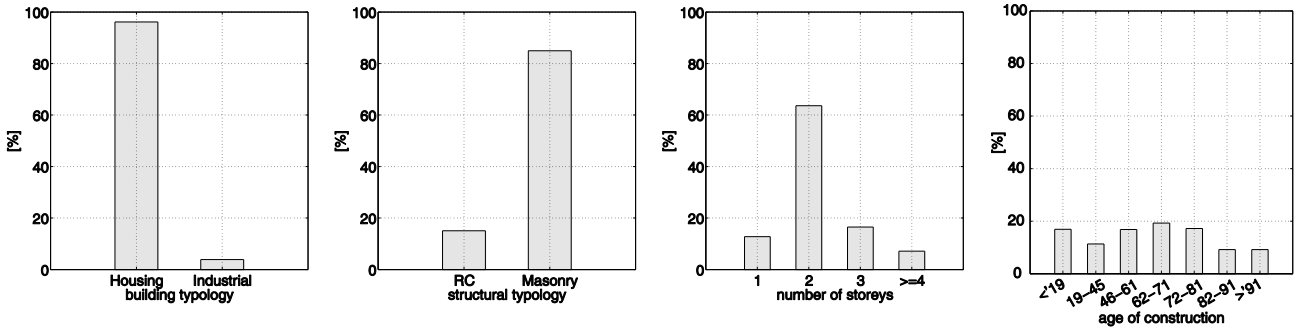

(a) (b) (c) (d)

Figure 1. Statistics for the 448 Municipalities hit by the earthquake of 20th of May 2012: building typology (a), structural typology (b), number of storeys (c), age of construction (d).

3. EVOLUTION OF THE SEISMIC CLASSIFICATION IN THE EMILIA REGION

In recent years, four are the fundamental dates for the evolution of the seismic classification in Italy: 1984, 1998, 2003, and 2008. In fact, after the Friuli (1976) and Irpinia (1980) disastrous earthquakes, three different seismic categories were set up, and the third category, characterized by a PGA equal to 0.04g, was introduced for the first time. First and second categories were characterized by a PGA equal to 0.10g and 0.07g, respectively (see Ricci et al., 2011). Such accelerations were determined through the seismic coefficient S equal to 12, 9, and 6, and decreasing with the increasing of the category form first to third. According to the latter classification (De Marco and Marsan, 1986) most of the area struck by the 2012 Emilia earthquake was classified as non seismic.

Successively, in 1998, a reclassification proposal was provided by the *Servizio Sismico Nazionale*. Such a classification was never adopted officially by any code but it is at the basis of the classification made in 2003 (OPCM 3274, 2003), after the San Giuliano earthquake. The 2003 regulation document introduced also modern design rules, such as the so called *capacity design*. On the other hand, it should be noted that these new design rules worked as recommendation, since they have never become compulsory, and it was still possible to design new structures according to the previous code (DM 16/01/1996), see Manfredi et al. (2013) for details.

According to 1998 classification the area struck by the 2012 earthquake was first classified as seismic, in the third category (PGA equal to 0.04g). Successively, according to the classification of the OPCM 3274, the whole area was still in third category; on the other hand a design PGA of 0.15g on rigid soil was employed, being the PGA with 10% exceeding probability in 50 years of such areas within the range 0.05-0.15g.
The last step in terms of seismic classification was made in 2008, when the DM 14/01/2008 was released. In the 2008 code the seismic input is based on specific hazard data based on a 5 km spaced grid (Stucchi et al., 2011) and spectral shape is site dependent, ending up in a code spectrum very close to a Uniform Hazard Spectrum (UHS). It should be finally noted that the 2008 code became the official Italian code and the only one to be employed only in July 2009, after the 2009 L'Aquila earthquake.
Based on the first seismic classification date and on statistical data about age of construction (Figure 1d) it is reasonable to assume that most of the buildings in the area struck by the 2012 Emilia earthquake were designed for gravity loads only.

Finally, a complete characterization of the seismic hazard in the area needs the definition of soil classification, given its influence on local amplification of events' PGA. Soil classification data, shown in Figure 2, highlight that most of the area struck by the earthquake is classified as D soil type. Information about soil classification are taken from SEE-GeoForm project (Di Capua et al., 2011), which provides an open source WebGis toolbox giving geological, geomorphological, geotechnical and geophysics data nationwide. Such information is further modified in order to consider for each census tract the predominant soil class.

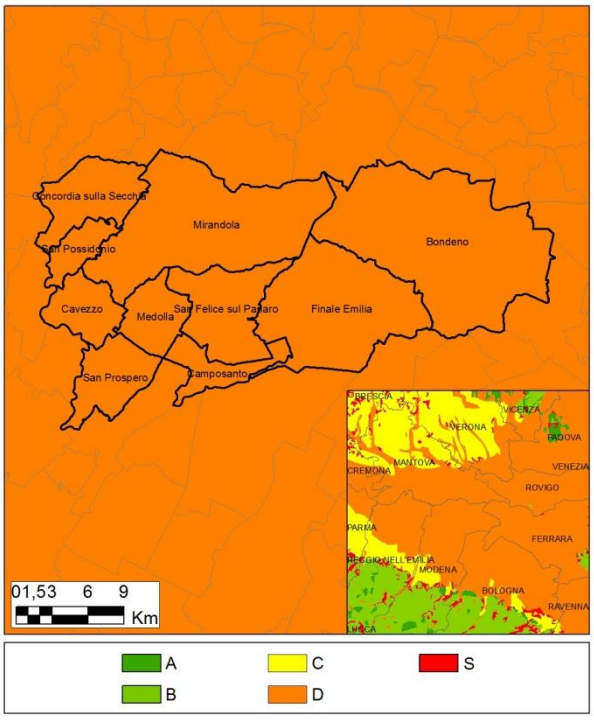

Figure 2. Soil classification on geological basis of the area struck by the earthquake.

4. EVENT AND DAMAGE

The Emilia 2012 sequence featured seven events of M_w higher than 5.0. These earthquakes were structurally damaging over a wide area. The events produced cumulative damage to structures (Iervolino et al., 2012). The M_w 6.0 mainshock occurred on the 20th of May 2012. In Figure 3 the shake map and epicenter coordinates (lat. 44.89; long. 11.23) are shown according to the information provided by INGV.

Observed damage was mostly registered on industrial precast buildings and masonry structures. Damage to RC buildings was relatively less severe. According to data collected during in-field survey right after the earthquakes of the 20th and the 29th of May (e.g., EPICentre Field Observation Report No. EPI-FO-200512, 2012; EPICentre Field Observation Report No. EPI-FO-290512, 2012; Parisi et al., 2012; Liberatore et al., 2013), it can be observed that RC buildings have been characterized by slight or moderate damage and only in rare situations structural collapses (EPICentre Field Observation Report No. EPI-FO-290512, 2012) have been observed.

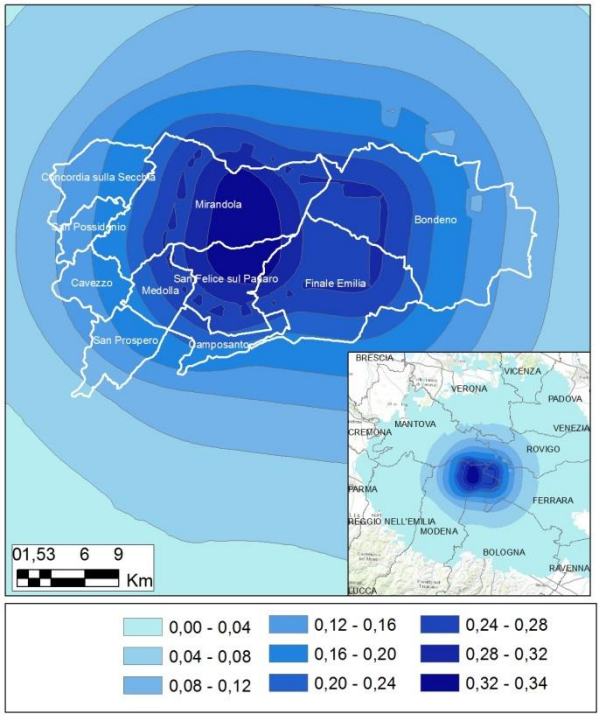

Figure 3. Shake map of the mainshock event occurred on the 20th of May 2012 and epicenter coordinates (lat 44.89; long. 11.23).

Most of observed damage affected non-structural elements. Seldom structural elements showed significant damage, and in most cases brittle failures occurred. Most of damage to RC structures was observed in the area close to the epicenters of the events of the 20th of May and the 29th of May, close to the towns of Mirandola, Cavezzo, San Felice sul Panaro. In Figure 4 to 10 an overview of structural and non-structural damage is collected. In Figure 4 two-, four- and five-storey RC buildings are shown; both buildings are located in the centre of Mirandola. Damage shown in Figure 4 can be classified as slight; in fact, in both cases the only plaster of the masonry infills is cracked. Such cases can be classified as the situations in which post event retrofitting interventions are very limited.

In Figure 5 an example of moderate damage to infills of a RC buildings in Mirandola is shown. Non-structural damage involved the external layer of the infill panels. In Figure 5(b) damage to the external layer allows the visual inspection of structural elements that did not show any damage.

Figure 6 shows a seven-storey building in which both structural and non-structural damage is observed. Damage to the external layer of infills, characterized by the crushing of the corners of the panels, is shown in Figure 6(a). Such damage seems a typical *corner crushing* failure of the infills. In the zoom-in shown in Figure 6(b) the diagonal cracking of the head of the columns adjacent to the damaged panel is shown. The 45° slope of the crack in Figure 6(b) suggests a brittle failure in the columns likely induced, on one hand, by the local interaction with the infill panels, and, on the other hand, by the poor local detailing of the element.

(a) (b)

Figure 4. Mirandola, slight damage to plaster on masonry infill panels (Parisi et al., 2012).

(a) (b)

Figure 5. Mirandola, moderate damage to the external layer of brick infills emphasizing the absence of damage to RC elements of the building (Parisi et al., 2012).

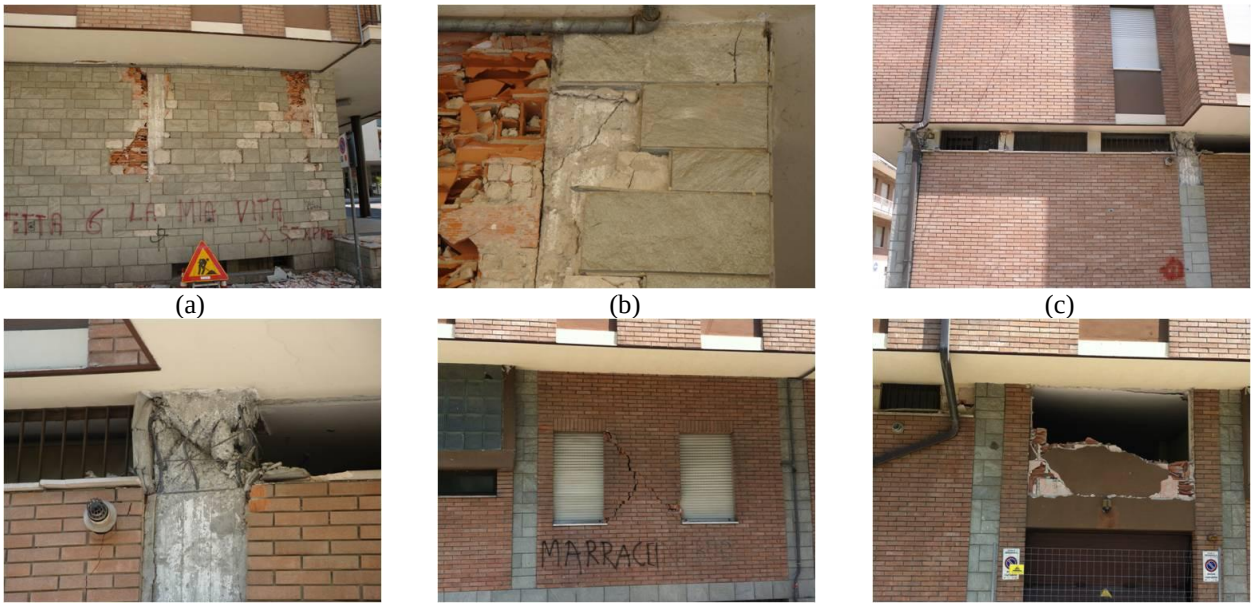

(a) (b) (c)

(d) (e) (f)

Figure 6. Mirandola, (a) damage to the external layer of the infill panels at the first storey of the building; (b) diagonal cracking characterized by shear failure at the top of the RC column; (c) structural damage in a squat RC column as a result of the local interaction between infill and RC elements because of the partial infilling, view of the façade of the building; (d) zoom-in of the squat column; (e) moderate damage and diagonal cracking of the infill panel between two openings; (f) significant damage and partial collapse of an infill panel; (Parisi et al., 2012).

Figure 6(c) and Figure 6(d) show the typical structural damage resulting from local interaction with infill panels. The openings and the partial infills in Figure 6(c) result in a reduced shear span ratio of the adjacent columns (*squat columns*); these kinds of structural situations, it is well known, favor the occurrence of brittle failures. The low percentage of transverse reinforcement shown in

Figure 6(d), 20 cm spaced stirrups, is not enough to guarantee the proper shear capacity (De Luca and Verderame, 2012) for the shear demand increased by the presence of partial infills. In fact, such stirrup spacing is very poor if compared to the actual prescriptions provided in Italian and European seismic codes (DM 14/01/2008; CEN, 2004) for this kinds of situations. In Figure 6(e) and Figure 6(f) examples of moderate and significant damage to infill panels are shown, respectively. In Figure 6(e) the diagonal cracking of the infill panel between two openings is shown; such kind of damage is very similar to the typical failure mode of structural panels in masonry structures. It is well known that openings in infill panels lead to a decrease in strength and stiffness of the panels also caused by the modification of stresses' transfer between infills and adjacent RC elements. The situation of the partially collapsed infill in Figure 6(f) recalls the typical collapse mechanism of sliding shear, characterized by cracking in the middle of the panel and a consequent out of plane failure of the top part of the infill (Shing and Mehrabi, 2002).

Figure 7 shows a detail of a RC column of a building in Cavezzo; damage occurred to the whole building can be classified as slight if the column shown is excluded. Figure 7(a) takes a typical concrete spalling at the corner of the rectangular section at the base of the column. The zoom-in of the base of the column provided in Figure 7(b) and 7(c) emphasizes a stirrup spacing equal to 20 cm and the typical buckling of the longitudinal bars caused by the poor transverse reinforcement that increases the unsupported length of the bar and consequently favors instability.

(a) (b) (c)

Figure 7. Cavezzo, RC column, (a) concrete spalling, (b) stirrup spacing equal to 20cm, (c) longitudinal bar buckling; (Parisi et al., 2012).

Figure 8 shows the first storey of a three-storey building in San Felice sul Panaro characterized by an irregular distribution of infill panels in height and plan (Liberatore et al. 2013). The zoom-in shown in Figure 8(a) and (b) suggests a collapse mode induced by the local interaction between infills and RC elements. Such kind of collapse, as it was already emphasized by Liberatore et al. (2013), is similar to damage observed after the 2009 L'Aquila earthquake (e.g., Verderame et al, 2011). The local interaction between infills and structural elements has increased the shear demand and, contemporarily, the poor seismic detailing of the transverse reinforcement has contributed to an inadequate capacity against brittle failures.

(a) (b)

Figure 8. San Felice sul Panaro, significant damage in RC elements because of local interaction with infill panels (Liberatore et al., 2013).

5. SEISMIC CAPACITY OF RC BUILDINGS

In order to generate damage scenarios for the Emilia earthquake, seismic fragility of the RC building stock must be evaluated. To this aim, benchmark structures are assumed as representative of the RC building stock struck by the earthquake.

A 2- and a 4-storey RC building are modeled and analyzed, which will be assumed in the following as representative of two vulnerability classes, namely – consistent with census data – RC buildings with three or less storeys and with four or more storeys, respectively. Based on the information previously discussed about the main features of RC buildings in the area (see Section 3), buildings are assumed as designed for gravity loads only.

5.1 Case study structures

The analyzed structures are symmetric in plan, both in longitudinal (X) and in transverse (Y) direction, with five bays in longitudinal direction and three bays in transverse direction. Interstorey height is equal to 3.0 m, bay length is equal to 4.5 m. Hence, the plan area is equal to (22.5×13.5) m^2. Slab way is always parallel to the transverse direction. Two- and four-storey buildings are considered, according to the typical number of storeys characterizing Emilia's RC building stock , with the same plan distribution of beams, columns and infill panels. Infill panels are uniformly distributed in all the external frames; their thickness is equal to 0.20 m and presence of openings is not taken into account. The geometric percentage of infilled area with respect to the global plan extension (ρ_w) is equal to 0.028 and 0.017 in longitudinal and transverse direction, respectively. Dead load is equal to 5.00 kN/m^2 and live load is equal to 2.00 kN/m^2. Mechanical properties for RC elements and infill panels are reported in Table 1.

	Mechanical property	μ	Reference
RC	Concrete compressive strength, f_c	25.0 MPa	(Verderame et al., 2001)
	Steel yield strength, f_y	369.7 MPa	(Verderame et al., 2012)
Infills	Shear elastic modulus, G_w	1240 MPa	(Fardis,1997;Rossetto and Elnashi,2005;Calvi et al.,2004)
	Young elastic modulus, E_w	4133 MPa	
	Shear cracking stress, τ_{cr}	0.33 MPa	
	Softening-to-elastic stiffness ratio, α	0.03	(Fardis,1997; Panagiotakos and Fardis, 1996)
	Residual-to-maximum stress ratio, β	0.01	

Table 1. Median values μ of mechanical properties – RC members and infills

5.1.1 Simulated design

Element dimensions are defined through a simulated design procedure for gravity loads only according to code prescriptions and design practices in force in Italy after World War II (Regio Decreto Legge n. 2229, 16/11/1939; Verderame et al., 2010a).

The structural configuration follows the parallel plane frames system: gravity loads from slabs are carried only by frames in longitudinal direction. Beams in transverse direction are not present in the internal frames. Element dimensions are calculated according to the allowable stresses method; the design value for maximum concrete compressive stress is assumed equal to 5.0 and 7.5 MPa for axial load and axial load combined with bending, respectively. Column dimensions are calculated according only to the axial load based on the tributary area of each column; beam dimensions and reinforcement are determined from bending due to loads from slabs. Reinforcing bars are smooth and their allowable design stress is equal to 160 MPa. Section dimensions are (0.30×0.50) m^2 for beams, whereas they are variable for columns, depending on the design axial load.

5.2 Seismic capacity

The analysis approach followed for the evaluation of the seismic capacity of benchmark structures is described herein. The non linear modeling approach for RC elements and infill panels is shown, and the employed strength reduction factor-ductility-period (R-μ-T) relationship is discussed.

5.2.1 Modelling

Nonlinear response of RC elements is modeled by means of lumped plasticity: beams and columns are represented by elastic elements with nonlinear rotational hinges at the ends. A three-linear envelope is used; characteristic points are cracking, yielding and ultimate. The behavior is assumed linear elastic up to cracking and perfectly-plastic after yielding. Section moment and curvature at cracking and yielding are calculated on a fiber section, for an axial load value corresponding to gravity loads. Rotation at yielding is evaluated through the formulations given in (Biskinis and Fardis, 2010).

Infill panels are modeled by means of equivalent struts. Modeling infills through single compressed struts allows to investigate the effect of the panels on the global behavior of the analyzed structure. It is to be noted that possible brittle failure due to local interaction between infill panels and the surrounding RC elements is beyond the purpose of this paper. The adopted model for the envelope curve of the force-displacement relationship is the model proposed by Panagiotakos and Fardis (1996), shown in Figure 9. For further details, the reader is referred to (Ricci et al., 2013), where the same model was employed and described in detail.

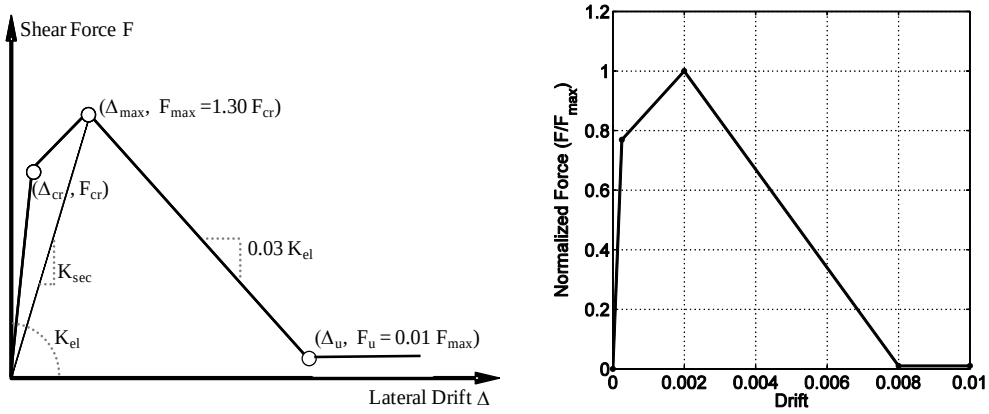

Figure 9. Single strut model (Panagiotakos and Fardis, 1996)

5.2.2 Analysis methodology

Nonlinear Static Push-Over (SPO) analyses are performed on the benchmark buildings both in X and Y direction: the assumed lateral load pattern is proportional to the displacement shape of the first mode and lateral response is evaluated in terms of base shear-top displacement relationship. Structural modeling and numerical analyses are performed through the "PBEE toolbox" software (Dolšek, 2010), combining MATLAB® with OpenSees (McKenna et al., 2004), modified in order to include also infill elements (Ricci, 2010; Celarec et al., 2012).

The lateral response is characterized by a strength degradation due to infill failure; thus a multi-linearization of the pushover curve is necessary and it is carried out by applying the equal energy rule between the pushover curve and the multi-linearized curve.

Starting from the multi-linearized capacity curves, IN2 curves (Dolšek and Fajfar, 2008) for the equivalent SDoF systems are obtained by assuming as Intensity Measure (IM) both the elastic spectral acceleration at the period of the equivalent SDoF system, $S_{ae}(T_{eff})$, and the PGA.

Values of $S_{ae}(T_{eff})$ and PGA corresponding to characteristic values of displacement (ductility), including the considered Damage States (DSs) analyzed in the following, are calculated, based on

the R-μ-T relationships given in (Dolšek and Fajfar, 2004) for degrading response. It is worth noting that this relationship is intended to be used with an idealized Newmark-Hall type elastic spectrum. In the proposed R-μ-T relationship, the ductility (μ) is a piecewise linear function of the strength reduction factor (R); the relationship depends on the effective period of the structure, the minimum-to-maximum strength ratio r_u, and the characteristic periods of the ground motion T_C and T_D (Dolšek and Fajfar, 2004). The ductility at the beginning of degradation μ_s and the residual-to-maximum strength ratio r_u are essential for the proposed R-μ-T relationship. Hence, the IN2 curves are strictly dependent on the parameters μ_s and r_u of the multi-linearized capacity curves. Moreover, the procedure proposed in (Dolšek and Fajfar, 2005) to improve the accuracy of the displacement demand assessment in the case of low seismic demand is applied.

Spectral shape used for the construction of the IN2 curves are the demand spectra adopted in Eurocode 8 – type I for D soil class (see Section 2), and the obtained PGA capacities are horizontal accelerations that already include local amplification due to soil effects. In the next Section, the analyzed Damage States and the corresponding displacement capacities are described; seismic intensity corresponding to each Damage State can be obtained through IN2 curves.

5.3 Damage States

In the previous Section, a tool to obtain the relationship between an IM (e.g. PGA) and an EDP (e.g. top displacement demand) was shown through IN2 curves. In this Section, capacities corresponding to different Damage States (DSs) are defined in order to generate a large-scale damage scenario starting from the seismic input provided by the shake map of the event and, finally, to carry out a comparison between the simulated damage scenario and post-event damage.

Local displacement capacity limits must be introduced in order to describe the evolution of the damage with increasing displacement in structural and non-structural members on a mechanical basis. The attainment of these local displacement capacity limits implies the overcoming of the corresponding DSs. In particular, the local limit capacities correspond to *top displacement* threshold values on the pushover curve of the structure and IM values on the IN2 curves.

It is worth noting that local limit capacities should be properly related to observed damage rather than to Limit State definitions provided by code, in order to properly linking the introduced DSs to the typical observed damage after earthquakes. Starting from the end of XIX century, different seismic intensity scales have provided a relationship between observed damage and seismic intensity, by defining the magnitude of an earthquake on the basis of the damage to structures: the Mercalli scale, with its following versions, (e.g. the Mercalli-Cancani-Sieberg scale), and the most recent EMS-98 Macro-seismic scale (Grünthal, 1998).

In particular, the EMS-98 scale defines five DSs, from *slight* damage up to *destruction*, passing trough *moderate*, *heavy* and *vey heavy* damage. For each DS, the damage to both structural and non structural components is described, for both RC buildings (see Figure 10) and masonry buildings.

It is worth noting that it is necessary to associate to the description of the damage for each DS provided by the EMS-98 scale a *local displacement capacity limit*, in order to investigate the achievement of each DS on the analyzed numerical model of the structure and to evaluate the corresponding PGA capacity through IN2 curves. The conversion of the observed damage described on RC buildings at each DS into local displacement capacity limits is reported in Figure 10 and explained below.

DS1	DS2	DS3	DS4	DS5
			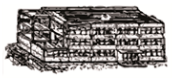	
Grade 1: Negligible to slight damage *(no structural damage, slight non-structural damage)*	**Grade 2: Moderate damage** *(slight structural damage, moderate non-structural damage)*	**Grade 3: Substantial to heavy damage** *(moderate structural damage, heavy non-structural damage)*	**Grade 4: Very heavy damage** *(heavy structural damage, very heavy non-structural damage)*	**Grade 5: Destruction** *(very heavy structural damage)*
Fine cracks in plaster over frame members or in walls at the base. Fine cracks in partitions and infills	Cracks in columns and beams of frames and in structural walls. Cracks in partition and infill walls; fall of brittle cladding and plaster. Falling mortar from the joints of wall panels	Cracks in columns and beam column joints of frames at the base and at joints of coupled walls. Spalling of concrete cover, buckling of reinforced rods. Large cracks in partition and infill walls, failure of individual infill panels	Large cracks in structural elements with compression failure of concrete and fracture of rebars; bond failure of beam reinforced bars; tilting of columns. Collapse of a few columns or of a single upper floor	Collapse of ground floor or parts (e. g. wings) of buildings
$\min\left(\Delta_{cr}^{inf};\Delta_{cr}^{RC}\right)$	$\min\left(\Delta_{max}^{inf};\Delta_{y}^{RC}\right)$	$\min\left(\Delta_{ult}^{inf};\Delta_{spalling}^{RC};\Delta_{buckling}^{RC}\right)$	Δ_{ult}^{RC}	Δ_{coll}^{RC}

Figure 10. Classification of damage for RC structures in EMS-98 scale and corresponding interpretation in the numerical structural model; adapted from (Grünthal, 1998) - (inf: *infills*; RC: *Reinforced Concrete elements*).

The definition of the DSs has been carried out interpreting the qualitative terms used by EMS-98 (e.g., *fine cracks*, *cracks* and *large cracks* for structural and non-structural components) into displacement thresholds related to non linear behavior of RC members and infills. A building can be classified in:

- Grade 1 (DS1) if it exhibits fine cracks in plaster over frame members or in infill panels. This condition corresponds in the mechanical model to the overcoming of the minimum between the cracking displacement in the envelope of infills and the cracking displacement in the envelope of columns.
- Grade 2 (DS2) if it is characterized by an increasing level of damage, cracks in RC members and infills. This DS can be associated to the achievement of the minimum between the displacement corresponding to the maximum strength in infills and the displacement corresponding to the first yielding in RC members.
- Grade 3 (DS3) if it is characterized by cracks in RC members, large cracks in infills and partitions or failure of infills, spalling of concrete cover and buckling of steel bars. Thus, DS3 can be associated to the overcoming of the minimum between the displacement corresponding to spalling of the concrete cover (Berry and Eberhard, 2005), the displacement corresponding to the buckling of steel bars (Berry and Eberhard, 2005) and the displacement corresponding to the end of the degrading branch in the envelope of infill panels (i.e. "infill failure").
- Grade 4 (DS4) if it shows large cracks in structural elements with compression failure of concrete, bond failure of beam longitudinal bars or collapse of a few columns. This displacement threshold is assumed to correspond to a 20% decrease in flexural strength of columns (Panagiotakos e Fardis, 2001). Hence, this capacity threshold is defined by a displacement corresponding to a resistance degradation of 20% of the peak resistance on the tri-linear backbone curve proposed by (Haselton et al., 2008). Note that such model was calibrated on a database of RC elements that are not representative of existing RC buildings in Italy; nevertheless, for elements with smooth bars such "ultimate" rotation can be assumed to be equal to that of elements designed according to contemporary seismic provisions (Verderame et al., 2010b).
- Grade 5 (DS5) if it is characterized by the collapse of the whole structure or its parts. In the numerical model, the achievement of this DS is assumed as corresponding to the overcoming of the displacement corresponding to zero shear strength in columns in the adopted model, taking into account P-Delta effects in the degrading branch of the envelope curve.

Figure 11 shows IN2 curves both in terms of $S_{ae}(T_{eff})$ and PGA for the 2- and the 4-storey analyzed buildings. $S_{ae}(T_{eff})$ and PGA capacity at each DS is represented on IN2 curves.

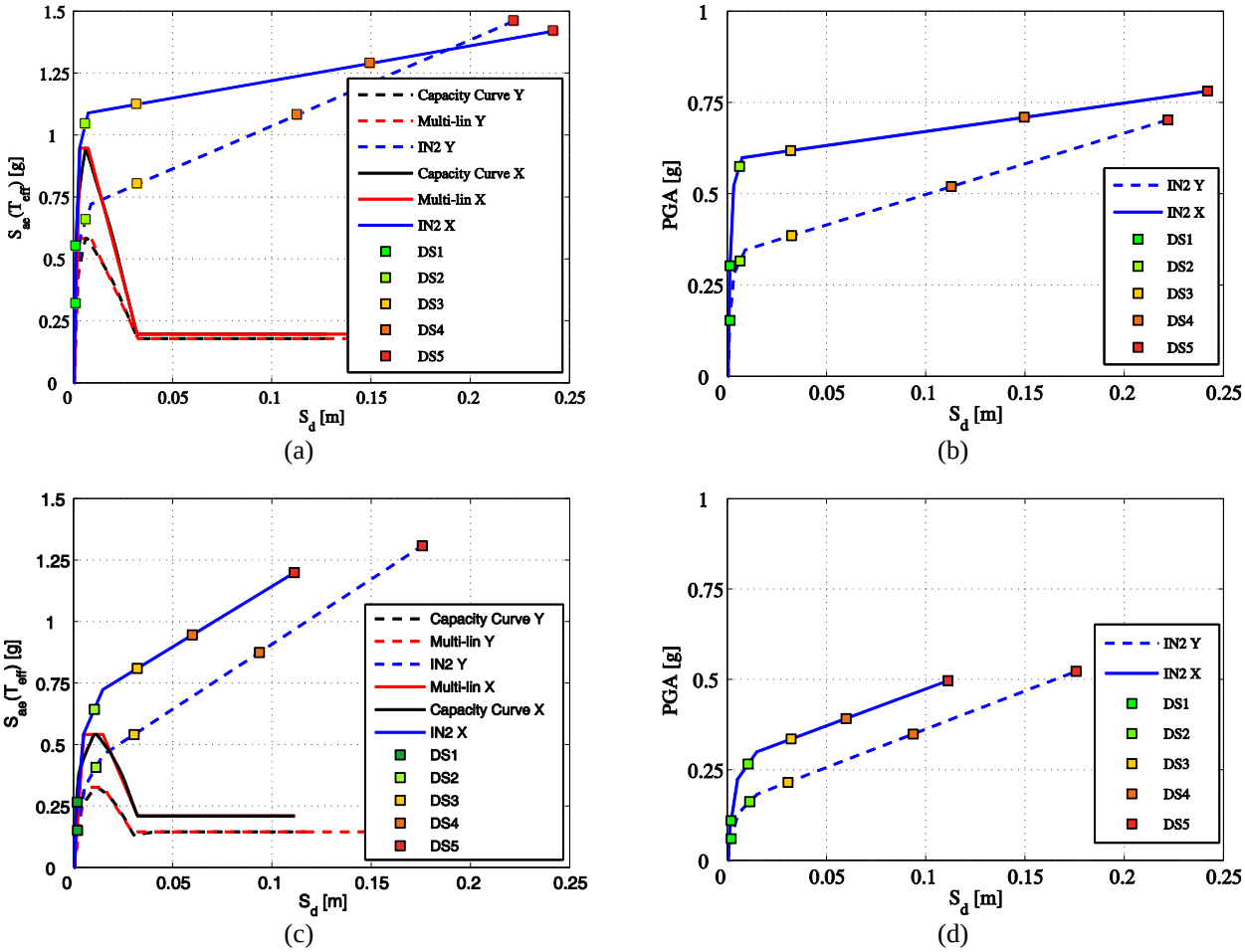

Figure 11. Capacity curves, multi-linearized capacity curves, IN2 curves in terms of $S_{ae}(T_{eff})$ and PGA for the 2-storey (a, b) and 4-storey (c, d) benchmark structures.

6. FRAGILITY ANALYSIS

In order to analyze the seismic capacity of the benchmark structures, materials and modeling variability has to be considered. Hence, fragility curves at the described DSs are obtained. First of all, the methodology used for the evaluation of fragility curves is illustrated.

A fragility curve represents the relationship between a seismic intensity parameter and the corresponding probability of exceedance of a given damage threshold (typically represented by a displacement capacity). If PGA capacity at a given DS is attained in a population of buildings, the cumulative frequency distribution of these observations provides the fragility curve (based on PGA seismic intensity measure) for that population of buildings at that DS.

Herein, the population of buildings is generated by a number of samplings of Random Variables, which are input parameters to the determination of the PGA capacity (e.g., material characteristics or capacity parameters), defined by Probability Density Functions (PDFs) describing the expected values and the corresponding variability, according to a Monte Carlo simulation technique. A stratified sampling of Random Variables is executed through the Latin Hypercube Sampling (LHS) technique (McKay et al., 1979), assuming a "median" sampling scheme (Vorechovsky and Novak, 2009). Nevertheless, it would be too computationally demanding to carry out a specific SPO analysis (for calculating the PGA capacity) for each sample of the chosen Random Variables. Hence, a Response Surface Method (RSM) is applied (Pinto et al., 2004), assuming a second-order polynomial relationship between the PGA capacity, assumed as the scalar

output variable, and the selected Random Variables, assumed as input variables. The design of experiments needed to determine such relationship is carried out according to the Central Composite Design (CCD) method. Hence, the number of experiments adds to n=1+2k+2k, if k input variables are assumed.

The assumed input Random Variables (RVs) are: concrete compressive strength, f_c; steel yield strength, f_y; chord rotation at yielding in RC members, θ_y; chord rotation at capping in RC members, θ_{cap}; post-capping chord rotation in RC members, θ_{pc}; "Loads" of load-displacement relationship of the infill trusses; F_{infill}; and, "Displacements" of load-displacement relationship of the infill trusses, D_{infill}. The variable F_{infill} is a vector whose components are [F_{cr}; F_{max}], where F_{cr} and F_{max} are cracking and maximum strength of infills, respectively; similarly, the variable D_{infill} is the vector [D_{cr}; D_{max}], where D_{cr} and D_{max} are cracking and maximum displacement of infills, respectively. Residual strength and corresponding displacement of infills are obtained from F_{infill} and D_{infill} according to the adopted model (Panagiotakos and Fardis, 1996). Inelastic displacement demand evaluated from R-μ-T relationship is assumed as a Random Variable, too: uncertainty in inelastic displacement demand, in a spectral assessment method framework, is due to the record-to-record variability observed in the results of the nonlinear dynamic analyses carried out on SDoF systems (with several records) employed to obtain the R-μ-T relationships. Hence, the value of the inelastic displacement demand calculated by means of the given R-μ-T relationship is assumed as the median value, and the corresponding variability is estimated according to (Dolšek and Fajfar, 2004). The number of experiments, i.e. the number of static pushover analyses carried out to evaluate PGA capacity, adds to $n=1+2\cdot7+2^7=143$ for each case study, in each direction.

RV	Distribution	$\bar{\mu}$	CoV	Reference
f_c	Lognormal	1	0.31	(Verderame et al., 2001)
f_y	Lognormal	1	0.08	(Verderame et al., 2012)
θ_y	Lognormal	1.015	0.331	(Biskinis and Fardis, 2010)
θ_{cap}	Lognormal	1	0.54	(Haselton et al., 2008)
θ_{pc}	Lognormal	1	0.72	(Haselton et al., 2008)
F_{infill}	Lognormal	[1;1]	[0.30;0.30]	(Fardis,1997;Rossetto and Elnashai,2005;Calvi et al.,2004)
D_{infill}	Lognormal	[1;1]	[0.30;0.70]	(Fardis,1997;Rossetto and Elnashai,2005;Calvi et al.,2004)
μ	Lognormal	1	0.70	(Dolšek and Fajfar, 2004)

Table 2. Distribution, normalized median ($\bar{\mu}$) and CoV values for the selected RVs

In order to apply the illustrated procedure, a lognormal distribution is assumed for each RV, and corresponding CoVs are defined according to literature studies; the considered input variables normalized to their median values are represented in Table 2.

The resulting PGA capacity data allow estimating the second-order polynomial relationship between the PGA capacity and the assumed Random Variables. Subsequently, a LHS of the k=7 considered Random Variables is carried out, thus obtaining m sets of values of these variables. In particular, m=1000 samplings are executed. The m×k obtained sampling matrix is used to estimate, through RSM, the corresponding m values of PGA capacity.

The corresponding cumulative frequency distributions of the obtained PGA capacity values provide the fragility curves for the benchmark structures in X and Y directions at each DS. Results are illustrated in the following (Figure 12(a), (b)). In the same way, fragility curves independent on the direction can be obtained (see Figure 13), through the evaluation of the cumulative frequency distribution of the minimum PGA capacities between X and Y direction for each sampling.

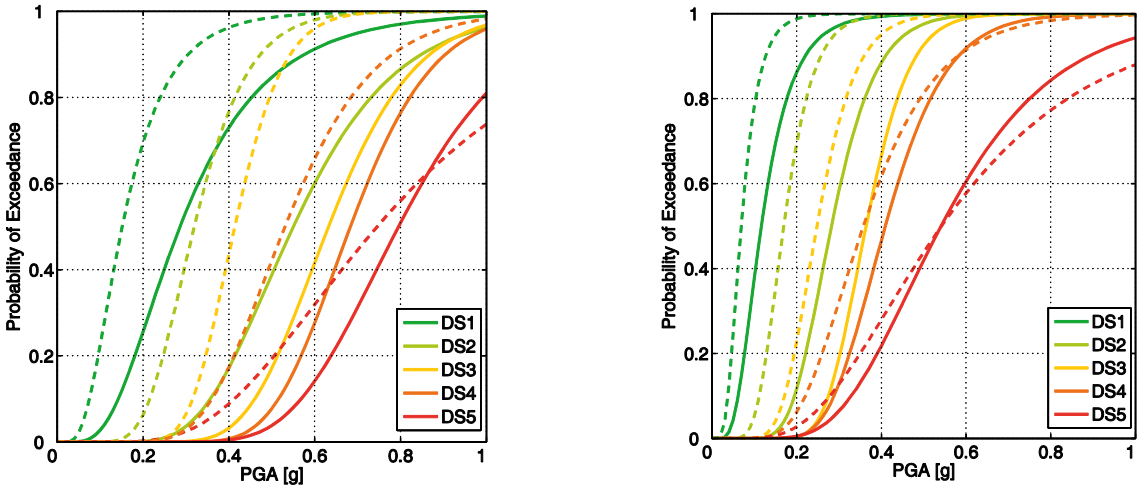

(a) (b)

Figure 12. Fragility curves – 2-storey (a) and 4-storey building (b) in longitudinal (solid line) and transversal (dashed line) direction

The logarithmic standard deviation of PGA capacity (β) provides a useful indication about the overall sensitivity of seismic capacity to the variability of the parameters mainly influencing the seismic response. Table 3 shows the estimated median (μ_{PGA}) and logarithmic standard deviation (β_{PGA}) of PGA capacity for each case study building.

		DS1		DS2		DS3		DS4		DS5	
		μ_{PGA}	β_{PGA}	μ_{PGA}	β_{PGA}	μ_{PGA}	β_{PGA}	μ_{PGA}	β_{PGA}	μ_{PGA}	β_{PGA}
2-storey	X	0.29	0.55	0.55	0.34	0.63	0.25	0.68	0.22	0.80	0.26
	Y	0.15	0.55	0.32	0.31	0.41	0.21	0.53	0.30	0.75	0.46
	indip	0.15	0.55	0.32	0.31	0.41	0.21	0.52	0.26	0.68	0.33
4-storey	X	0.12	0.49	0.28	0.29	0.36	0.22	0.41	0.27	0.54	0.39
	Y	0.07	0.47	0.17	0.33	0.25	0.29	0.36	0.38	0.54	0.52
	indip	0.07	0.47	0.17	0.32	0.25	0.28	0.35	0.34	0.51	0.44

Table 3. Median (μ_{PGA}) and logarithmic standard deviation (β_{PGA}) of PGA capacity

It can be observed that the value of β decreases from DS1 to DS3 and then increases again from DS3 up to DS5, for each case study building and in both directions.

At DS1, the relatively low slope of the fragility curve, i.e. the higher values of the parameter β, reflects the particularly high influence of the uncertainty in mechanical properties of infill panels, in terms of strength and stiffness, on the seismic capacity. A sensitivity analysis was also carried out in order to highlight the essential influence of the RVs D_{infill} and F_{infill} on the seismic response in terms of PGA capacity. In particular, at DS1, 2-storey building is more affected by infill mechanical properties with respect to 4-storey building, resulting in a higher value of β.

When damage of the structure moves from DS1 to DS3, the influence of D_{infill} and F_{infill} on the seismic response gradually decreases, and, in turn, the value of β decreases. Moreover, a decreasing variability in seismic capacity from DS1 to DS3 can be explained with a reduction in the slope of IN2 curves with increasing displacement, which leads, for higher DSs, to a lower dispersion in PGA capacity given equal the dispersion in displacement capacity.

The variability in the seismic response at DS4 and DS5 is mainly due to the variability in the response of RC members. Variability in displacement capacity thresholds at DS4 and DS5 is strictly influenced by the variability in post-capping chord rotation capacity (CoV=72%), the latter more than the former. Moreover, the values of β related to the fragility curves independent on the

direction are very close to the corresponding values of β obtained for the fragility curves in transverse (Y) direction.

6.1 Simulation of damage scenarios

In this Section, the adopted procedure for obtaining damage scenarios for the RC building population struck by the Emilia earthquake is described, based on the fragility analysis previously illustrated, on building stock characteristics evaluated from census data, and on spatial distribution of seismic demand provided by the shake map of the event. Damage scenario is evaluated for Municipalities within the epicentral area.

Figure 13 shows the damage distribution related to determined PGA ranges for 2- and 4-storey case study buildings (in Figure 13 the tick label on x-axis represents the upper bound of the corresponding range) together with the fragility curves at each DS independent of the direction – which were obtained as explained above.

It can be observed that the damage to the 2-storey building is essentially related to cracking in structural or non structural components (DS1-DS2). Only when PGA values are higher than 0.30g infill panels failures, concrete cover spalling or buckling of steel bars appear (DS3).

On the contrary, the 4-storey building exhibits a higher vulnerability, leading higher damage levels, showing also a quite significant rate of structural collapses (DS4-DS5) when PGA is higher than 0.20g.

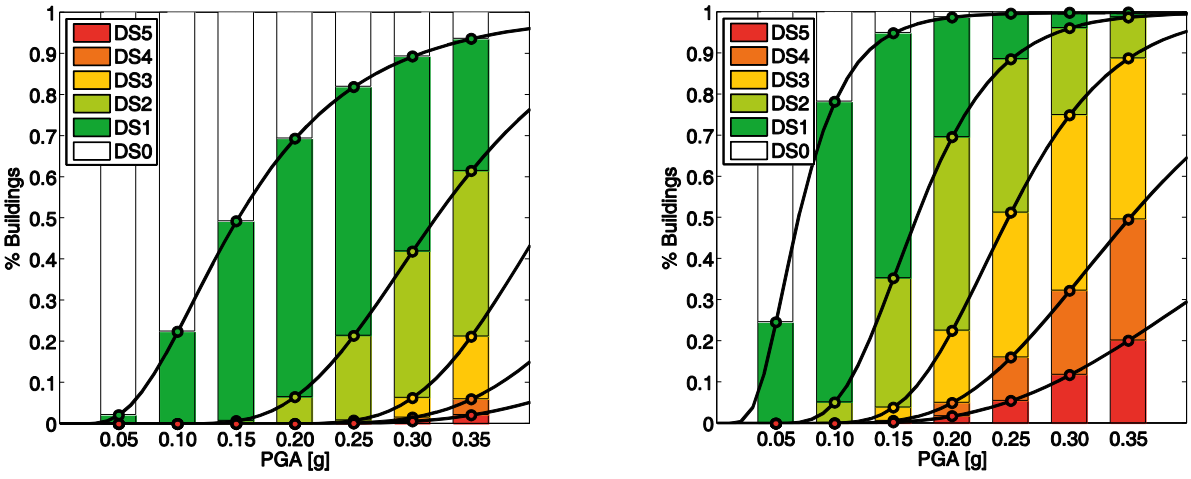

(a) (b)

Figure 13. Fragility curves independent of the direction and damage scenarios related to 2- (a) and 4- (b) storey buildings depending on PGA values.

These fragility curves are used to estimate the distribution of the expected damage to the RC building stock. To this end, two vulnerability classes can be identified; one characterized by a number of storeys equal or lower than three, whose structural response is assumed equal to that of the 2-storey benchmark structure, and the other one characterized by a number of storeys equal or greater than four, whose structural response is assumed equal to that of the 4-storey benchmark structure. Based on this assumption, the expected damage distribution in each census tract can be evaluated as the weighted average of the expected damage distribution for each one of the two vulnerability classes defined above, depending on their respective percentage of occurrence within the census tract, and, of course, on the PGA demand provided by the shake map of the event.

The estimation of the number of buildings in each vulnerability class for each census tract is based on data on building stock characteristics provided by census data, which are described in the following. Figure 14(a) shows percentages, for each Municipality, of the structural typology provided by the ISTAT (2001). The analyzed area is characterized by a very high percentage

(approximately 85% of the whole sample) of masonry buildings. In Figure 14(a), an information about the total number of buildings for each Municipality is provided through the size of the pies. Moreover, in each Municipality the ratio between the number of RC and masonry buildings reflects data shown in Figure 1; in fact, the percentage of RC buildings seldom overcomes 20% of the whole sample. In the area in which a PGA higher than 0.04g was registered, 90% of the buildings are masonry buildings, while this percentage is approximately equal to 80% where PGA was lower than 0.04g.

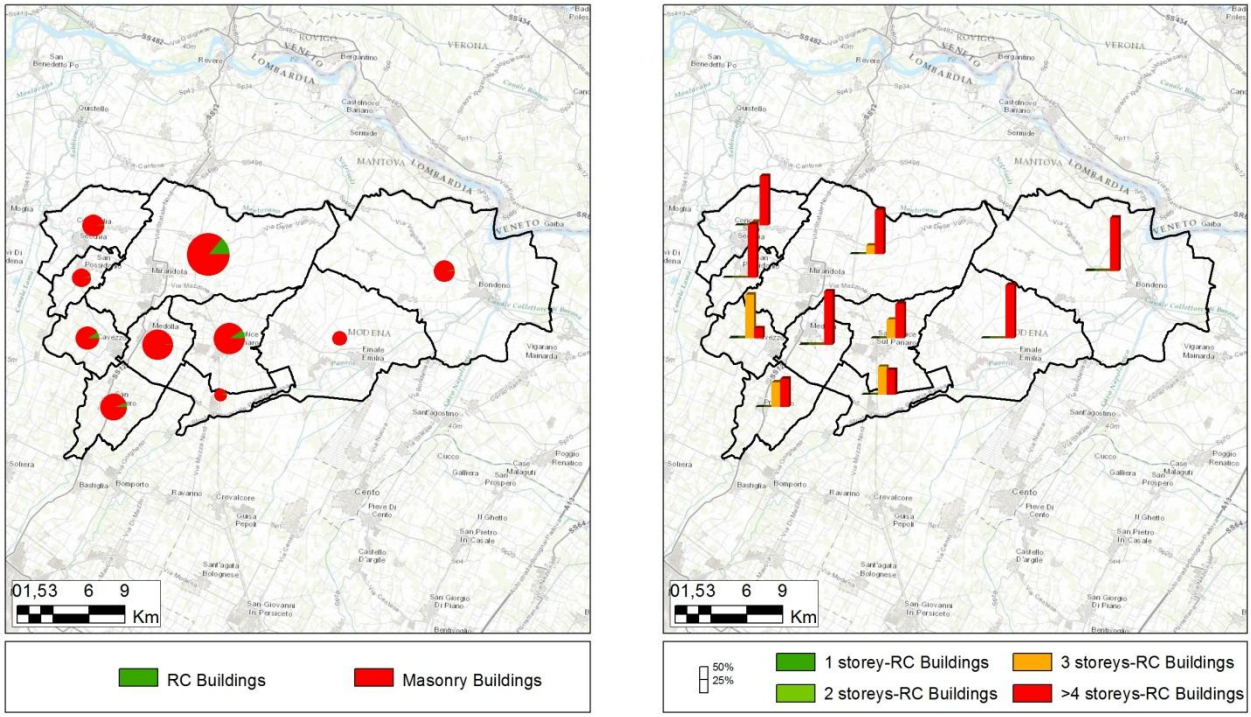

(a) (b)

Figure 14. Spatial distribution in each Municipality of the structural typology provided by ISTAT data (a) and the number of storeys estimated according to the assumed disaggregation hypothesis (b)

2001 ISTAT data provide aggregate information on building characteristics for each census tract. Therefore, it is necessary to introduce some assumptions in order to obtain disaggregate statistical distribution of the number of storeys for each structural typology. To this aim, a useful indication is provided in (GNDT, 2000), where it is stated that the modal value of number of storeys for masonry buildings nationwide is equal to 1-2 storeys, whereas it is equal to 3-4 storeys for RC buildings. Based on these data, in this study the distribution of number of storeys for RC buildings is evaluated assuming that they are the tallest within each census tract. Following this hypothesis, aggregate data on number of storeys and structural typology of buildings within each census tract can be crossed, finally providing an estimate of the distribution of number of storeys for RC buildings for each census tract. The obtained data, aggregated at Municipality level for an easier understanding, are shown in Figure 14(b). Note that in the epicentral area RC buildings are mainly characterized by a number of storeys equal or greater than four.

Once the distribution of the number of storeys for RC buildings is defined, the number of buildings belonging to each one of the two vulnerability classes represented by the benchmark structures – and the corresponding percentages of occurrence – are evaluated as *(i)* the sum of the number of RC buildings with three or less storeys and *(ii)* the number of RC buildings with four or more storeys, respectively.

The distribution of the expected damage to RC buildings can now be obtained, based on the PGA demand provided by the shake map of the event.

To this aim, if a single census tract lies on multiple shake map areas, a single PGA value is defined based on a weighted average. According to the evaluated value of PGA, the damage distribution for each vulnerability class can be evaluated from the respective fragility curves. Finally, according to the previously evaluated percentage of occurrence of such vulnerability classes, the expected damage distribution for each census tract can be obtained. Summing the values for all the census tracts within a Municipality, the damage scenario is obtained. Note that, although expected damage is obtained for each single census tract (thus allowing to use the most detailed data provided by census and to estimate with lower approximation the PGA demand at the site), in the following results will be shown for Municipalities, for an easier understanding. To this end, damage data are aggregated providing the expected percentage of RC buildings in each DS within each Municipality. The obtained damage scenario, corresponding to the mainshock of the 20th of May 2012, is shown in Figure 15.

According to the obtained scenario, RC buildings are characterized mainly by slight or moderate damage, and only in few cases structural collapses can be observed. In the areas far from the epicenter – characterized by a PGA value lower than 0.04g – the only expected damage consists of fine cracking on plaster or infill panels (DS1). In the epicentral areas, instead, severe damage is observed up to some rare collapses in the areas characterized by PGA value higher than 0.28g. Results are in fair accordance with the damage observed after the event and described in Section 4.

If the analyzed area is divided into two zones, based on the PGA demand, the following observations can be pointed out:

- the areas where PGA is lower than 0.04g are mainly (95%) characterized by no structural damage (DS0) or slight damage (DS1);
- in the areas struck by PGA values higher than 0.04g, 69% of the buildings show no structural damage (DS0), while 23% and 5% of the buildings exhibit slight damage (DS1) and moderate damage (DS2), respectively. Moreover, only 2% of the buildings are expected to show wide cracking in structural elements, or infills failure, or concrete cover spalling (DS3). Among the buildings located in the area closest to the epicenter, only 0.7% and 0.3% can be classified in DS4 and DS5, respectively.

It is worth noting that the hypothesis assumed in order to obtain information on building stock starting from aggregated census data leads to an (unavoidable) approximation in the estimation of expected damage. The hypothesis adopted herein consists of assuming that the number of storeys of RC buildings is equal or greater than the number of storeys of masonry buildings within the same census tract. Such hypothesis ("high-side" estimate) can lead to overestimate the actual number of storeys of RC buildings, and thereby to overestimate their seismic vulnerability as well. In the following, the possible consequences of such an assumption are illustrated by analyzing the damage distribution obtained according to the opposite hypothesis ("low-side" estimate), i.e., assuming that the number of storeys of RC buildings is equal or lower than the number of storeys of masonry buildings within the same census tract. Note that, consistent with census data about percentage of occurrence of the two structural typologies, the "true" damage distribution should necessarily fall within these two estimates.

Moreover, damage distributions obtained considering that all RC buildings within each census tract belong to the 2- or the 4-storey vulnerability class are reported, providing the lower and upper bound estimates of seismic vulnerability, respectively. They represent useful reference values for seismic vulnerability assessment. Nevertheless, they may be inconsistent with census data about percentage of occurrence of the two structural typologies; hence, they are reported in Italic in the following Tables.

The Municipalities of Mirandola and San Felice sul Panaro can be used for this comparison, since most of damage shown in Section 4 is localized there. Both Municipalities are in the epicentral zone, and the average PGA demand is equal to 0.29g and 0.31g, respectively. Moreover,

differences in building characteristics between these two Municipalities can lead to interesting observations.

In Mirandola, a predominance of low-rise RC buildings is observed (84.2% with three or less storeys and 15.8% with four or more storeys, according to the adopted disaggregation hypothesis). In this case, "low-side" and "high-side" damage estimates are quite close to each other, and both of them are very close to the "2-storey" estimate. Recalling that any damage estimate consistent with census data should be comprised between "low-side" and "high-side", independent of the adopted disaggregation hypothesis, we can conclude that the assumption followed in data disaggregation has a minor influence on the outcome of the estimate.

	DS0	**DS1**	**DS2**	**DS3**	**DS4**	**DS5**
2-storey	*12.6%*	*51.8%*	*31.3%*	*3.3%*	*0.6%*	*0.5%*
low-side	12.1%	50.0%	31.2%	4.7%	1.2%	0.8%
high-side (adopted)	10.5%	44.3%	30.8%	9.4%	3.1%	1.8%
4-storey	*0.1%*	*5.4%*	*25.9%*	*41.2%*	*17.4%*	*9.8%*

Table 4. Damage distribution estimates for Mirandola

In San Felice sul Panaro, percentages of RC buildings with three or less storeys and with four or more storeys are much closer to each other (44.9% and 55.1%, respectively, according to the adopted disaggregation hypothesis). Then, "low-side" and "high-side" estimates are much less close to each other, compared with Mirandola Municipality, leading to a stronger dependence of the results on the assumed disaggregation hypothesis.

	DS0	**DS1**	**DS2**	**DS3**	**DS4**	**DS5**
2-storey	*9.1%*	*42.5%*	*38.1%*	*7.6%*	*1.6%*	*1.0%*
low-side	9.1%	42.5%	38.1%	7.6%	1.6%	1.0%
high-side (adopted)	3.9%	20.0%	27.7%	27.1%	13.3%	8.0%
4-storey	*0.1%*	*2.7%*	*17.1%*	*42.2%*	*23.5%*	*14.3%*

Table 5. Damage distribution estimates for San Felice sul Panaro

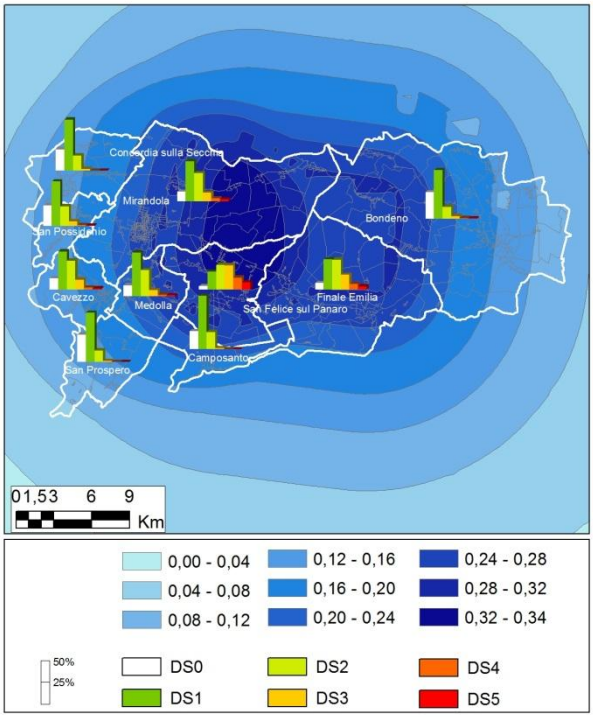

Figure 15. Spatial distribution in each Municipality of the damage for the mainshock of the 20th of May 2012

6.2 Some remarks about cumulative damage

During Emilia sequence the mainshock of the 20th of May was followed by another significant event of similar intensity (M_w=5.8, according to INGV) on the 29th of May. Damage to structures after the first event may have increased after the second event. An attempt to model this phenomenon, accounting for cumulative damage effect, has to be based on the evaluation of the residual capacity of damaged structures. This issue has raised a growing interest during last years (e.g. Luco et al., 2004; Bazzurro et al., 2006; Polese et al., 2013).

The damage scenario shown in the previous Section does not account for cumulative damage effect. In this Section, a simplified procedure for a fast evaluation of the cumulative damage to RC buildings is applied and a new damage scenario is presented.

First of all, the structural model characterized by the median values of all the Random Variables (Model#1) is analyzed for each benchmark structure. A conventional nonlinear SPO was already performed on the undamaged prototype structures and displacement values corresponding to DSs 1 to 5 were identified. For each DS the same nonlinear static analyses are carried out assuming that the structure is in that damage condition after the mainshock. SPO curves for the structure in its damaged state can be obtained by quasi-statically unloading the model from the ith damage state, DS_i, and reloading it re-imposing an increasing top displacement. The hypothesis of no degradation in strength and stiffness in the hysteretic behavior of both RC members and infill panels is assumed. Thus, SPO curves of the damaged structure return to, and follow the corresponding original pushover curves of the undamaged structure. Moreover, displacement capacity at each DS remains unchanged. Note that the SPO analyses for structures previously damaged in DS5 are not performed since it would be meaningless to model cumulative damage effects for structures that, according to the assumed damage scale, already attained the highest DS, and thereby will remain in this DS independent of the following events. Moreover, the pushover curve of a structure previously damaged in DS1 coincides with that of the undamaged structure, due to the definition itself of DS1 as limit of linear elastic structural (and non-structural) behavior.

It is worth noting that the residual displacement offset due to the unloading process is overestimated, due to the use of a static analysis procedure. Actually, the extent of this residual displacement is an artifact of applying a static procedure aimed at modeling the dynamic response

of the structure subject to ground motion: the residual displacement obtained from the SPO can be considered as an upper bound because the structure is not allowed to oscillate and return to a residual offset closer to its original position (Bazzurro et al, 2006).

This process leads to a family of SPO curves, two (one per orthogonal direction) for each DS. Then, starting from the SPO curves of the damaged structure for each DS, IN2 curves are obtained applying a proper R-μ-T relationship for degrading (Dolšek and Fajfar, 2004) or non-degrading (Vidic et al., 1994) structural systems aiming at estimating the residual capacity in terms of the (aftershock) ground motion intensity necessary to cause the achievement of each one of the higher DSs.

IN2 curves in terms of $S_{ae}(T_{eff,DS_i})$ – i.e. spectral acceleration obtained for damage state DS_i in terms of an oscillatory period T_{eff,DS_i} – and PGA are shown in Figure 16 for the 4-storey benchmark structure in its "weakest" direction (i.e., transverse).

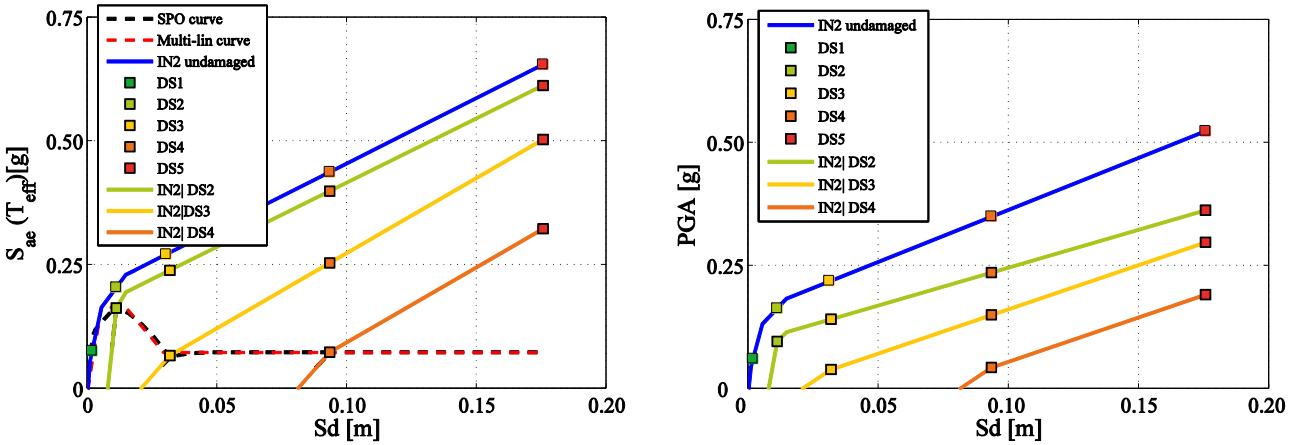

(a) (b)

Figure 16. IN2 curves in terms of $S_{ae}(T_{eff}DSi)$ (a) and PGA (b) for the 4-storey building in weak (transverse) direction

This residual capacity will strictly depend on the residual displacement offset measured after the mainshock; thus the overestimation of residual displacement will cause the underestimation of the residual ductility capacity and therefore a conservative assessment of residual seismic capacity.

For an expeditious evaluation of the fragility curves of the damaged structures, seismic capacity of Model#1 in terms of PGA is assumed equal to the new median capacity at DS_j given DS_i (with j>i), and the logarithmic standard deviation at each DS (β_{PGA}) is assumed equal to the corresponding value for the same DS for the undamaged structure. Hence new fragility functions are obtained at DS_j given DS_i (with j>i), as shown in Figure 17.

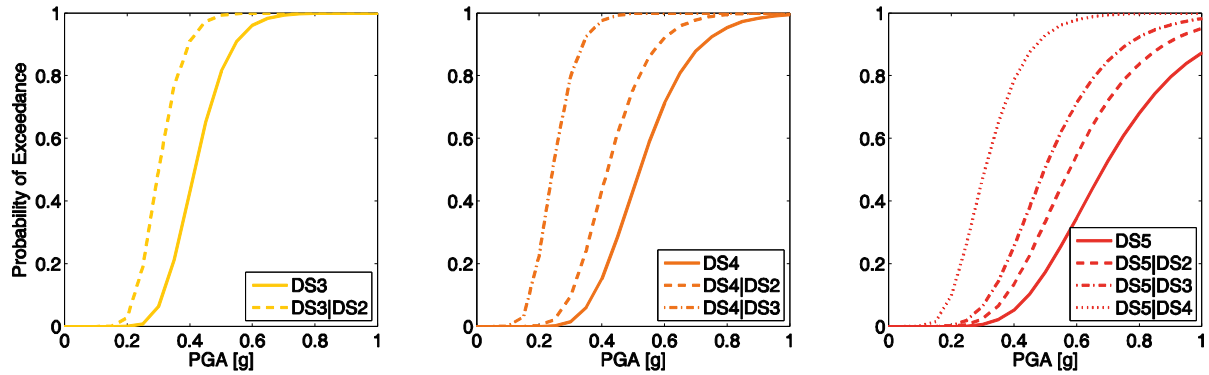

(a)

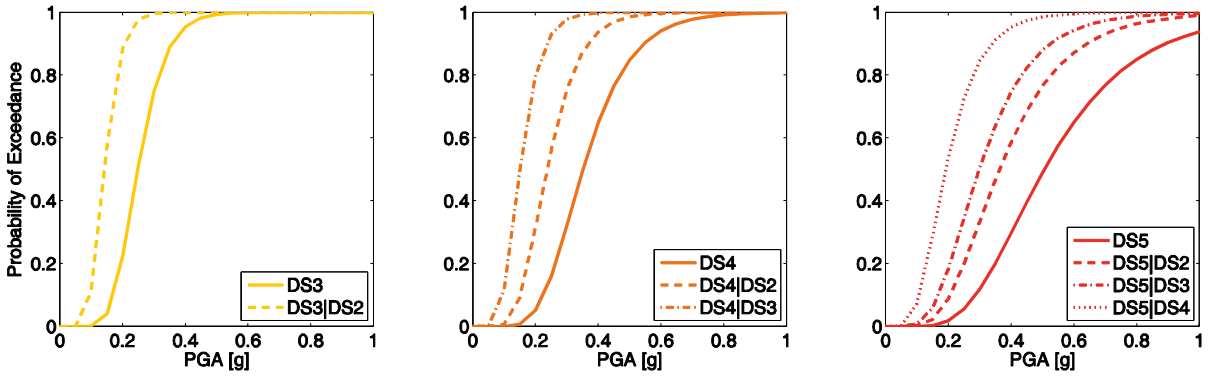

(b)

Figure 17. Fragility curves for the 2-storey (a) and 4-storey (b) building – independent on the direction at DS_j given DS_i (with j>i)

Based on the shake map of the event of the 29th of May (see Figure 18(a)), and based on the same assumptions made for the construction of the previous damage scenario, a new damage scenario is obtained, as shown in Figure 18(b).

The results of this procedure show that a certain percentage of buildings shifts from DS0 and DS1 to higher DSs, as expected, due to the reduced (residual) seismic capacity of a damaged structure and because of the higher values of PGA provided by the shake map of the event of 29th of May in some Municipalities. Such a percentage becomes higher for the Municipalities that are very close to the new epicenter, as expected. Note that Figure 18(b) shows the percentage of buildings in each DS with respect to the whole number of RC buildings.

The results of the scenarios in terms of the number of buildings in each DS are reported in Table 6 through *Cumulative Damage Matrices* (CDMs) for San Felice su Panaro, Mirandola, and Cavezzo: each row is related to a specific DS_i that was reached after the mainshock, and in each column the number of buildings that shift from DS_i to DS_j (with $j \geq i$) due to the aftershock is shown. The sum over the i-th row provides the number of buildings in DS_i after the mainshock, while the sum over the i-th column provides the number of buildings in DS_i after the aftershock. Based on their definition, CDMs are upper triangular matrices.

The new scenario seems to overestimate the number of buildings in DS4 and DS5 with respect to the observed damage. Such overestimation can be explained as a result of the conservative overestimate of the residual displacement offset, and of the assumption regarding the distribution of buildings in terms of number of storeys (see Section 6.1). However, even after the event of 29th May the most populated DSs are those associated to a lower level of damage.

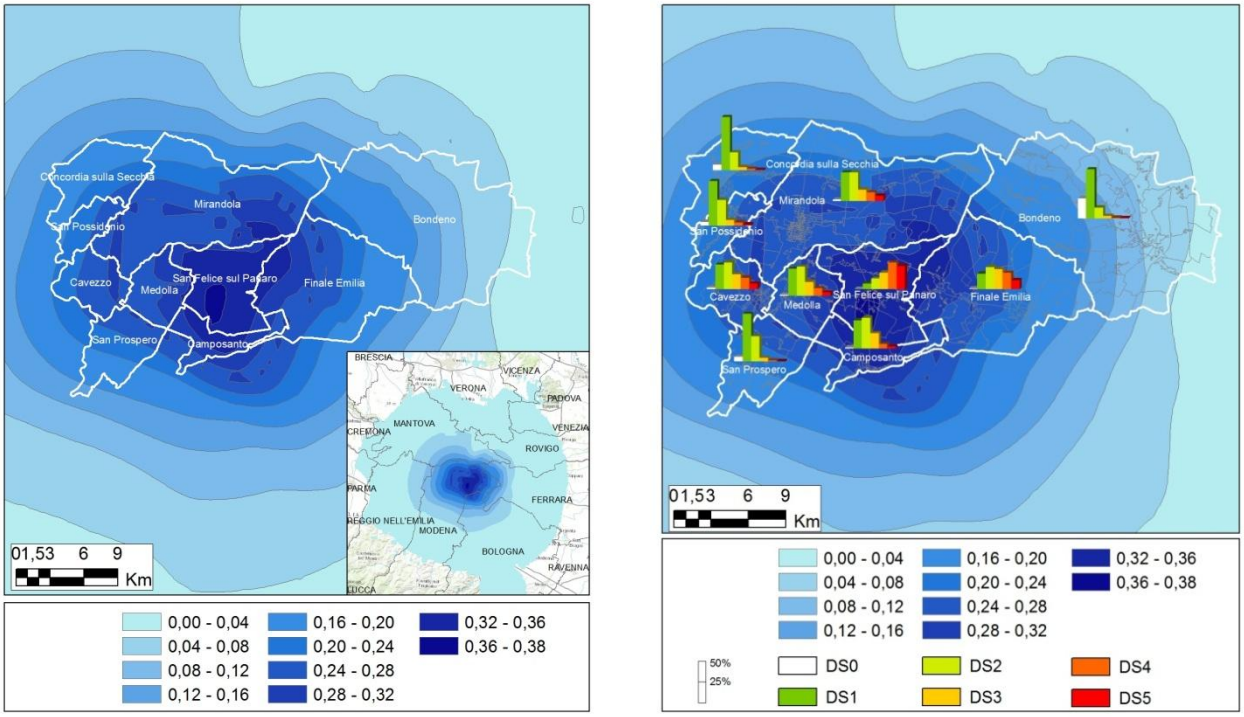

(a) (b)

Figure 18. Shake map of the event occurred on the 29th May (a) and partial distribution of the damage in each Municipality after that event (b)

(a)

20th May \ *29th May*	DS0	DS1	DS2	DS3	DS4	DS5
DS0	0	0	1	0	0	0
DS1		3	4	2	1	0
DS2			2	7	3	2
DS3				1	10	3
DS4					2	5
DS5						4

(b)

20th May \ *29th May*	DS0	DS1	DS2	DS3	DS4	DS5
DS0	5	20	11	1	0	0
DS1		104	46	6	2	1
DS2			66	33	8	4
DS3				8	21	4
DS4					6	6
DS5						7

(c)

20th May \ *29th May*	DS0	DS1	DS2	DS3	DS4	DS5
DS0	0	2	1	0	0	0
DS1		7	4	1	0	0
DS2			5	4	1	1
DS3				1	2	0
DS4					0	0
DS5						0

Table 6. CDMs for San Felice sul Panaro (a), Mirandola (b) and Cavezzo (c); the element CDM*(i,j)* represents the number of buildings in DS_i after the 20th May mainshock and in DS_j after the 29th May aftershock

7. CONCLUSIONS

The main features of the RC building stock that was struck by the Emilia 2012 earthquake and damage observed after the event were analyzed. Building stock characteristics and historical seismic classification were employed to carry out large-scale damage scenarios, which were finally compared with observed damage from in-field observations.

The evaluation of the seismic fragility was performed by means of numerical analyses carried out on benchmark structures that can be considered as representative of building classes. The adopted numerical model explicitly accounts for infills' contribution in strength and stiffness. Seismic fragility was evaluated at different Damage States, which explicitly took into account both structural and non structural damage, starting from a mechanical interpretation of Damage States defined according to EMS-98 scale.

Geo-referenced census data regarding the characteristics of the Emilia RC building stock and the seismic input provided by the shake map of the event were combined to carry out the large-scale damage scenarios. The simulated damage scenarios have shown the prevalence of slight or

moderate damage, mainly due to non structural components, and only in a few cases collapse occurred in the epicentral zone. The scenarios carried out seem to be in reasonable agreement with the observed damage.

The hypothesis assumed in order to obtain building stock characteristics from aggregated census data was described, and the influence of such assumption on damage estimation was discussed, depending on the characteristics of the building stock. These observations highlight another important issue about the generation of reliable large-scale damage scenarios, i.e., the need for comprehensive studies aimed at the statistical characterization of the existing building stock.

Given the peculiar character of Emilia seismic sequence, characterized by two relevant events (20^{th} and 29^{th} of may 2012), a preliminary cumulative damage scenario was carried out and, again, compared with in-field damage data. Notwithstanding the preliminary character of this final application, interesting results are still emphasized.

The comparisons shown represents a useful test-bed for future development of tools aimed at the evaluation of both seismic fragility and expected large-scale damage related to RC building stock.

REFERENCES

Bazzurro P, Cornell CA, Menun C, and Motahari M. (2006). Advanced Seismic Assessment Guidelines, Report Prepared for PG&E, PEER Lifelines Program, Task 507, September, 2006.

Berry, M.P. and Eberhard, M.O. (2005) "A Practical Performance Model for Bar Buckling," ASCE Journal of Structural Engineering, Vol. 131, No. 7, pp 1060-1070, July 2005.

Biskinis D. and Fardis M. N. (2010), Deformations at flexural yielding of members with continuous or lap-spliced bars. Structural Concrete 11(3): 128-138.

Calvi, G.M., Bolognini, D., Penna, A. (2004). Seismic Performance of masonry-infilled RC frames – Benefits of slight reinforcements. Invited lecture to "Sísmica 2004 - 6º Congresso Nacional de Sismologia e Engenharia Sísmica", Guimarães, Portugal, April 14-16.

Celarec, D., Ricci, P., Dolšek, M. (2012). The sensitivity of seismic response parameters to the uncertain modelling variables of masonry-infilled reinforced concrete frames. Engineering Structures, 35, 165-177.

CEN, 2004. European Standard EN1998-1:2004. Eurocode 8: Design of structures for earthquake resistance. Part 1: general rules, seismic actions and rules for buildings. Comité Européen de Normalisation, Brussels.

Chioccarelli E, De Luca F, Iervolino I. (2012), Preliminary study of Emilia (May 20th 2012) earthquake ground motion records V2.11, available at http://www.reluis.it.

Decreto Ministeriale del 14/1/2008. Approvazione delle nuove norme tecniche per le costruzioni. G.U. n. 29 del 4/2/2008.

Decreto Ministeriale del 16/1/1996 (1996) Norme tecniche per le costruzioni in zone sismiche. *Gazzetta Ufficiale della Repubblica Italiana,* 29 del 5/2/1996 (in Italian)

De Luca F. and Verderame G.M. (2012). A practice-oriented approach for the assessment of brittle failures in existing RC elements, Engineering Structures, DOI: 10.1016/j.engstruct.2012.09.038

De Marco R., Marsan P. (Eds.). (1986). Atlante della classificazione sismica del territorio nazionale, Servizio Sismico del Consiglio Superiore dei Lavori Pubblici, Istituto Poligrafico e Zecca dello Stato Italiano, Roma.

Di Capua G., Peppoloni S., Amanti M., Cipolloni C., Conte G., Avola D., Del Buono A., Negri Arnoldi C., Borgomeo E., (2011). Il Progetto SEE-GeoForm: uno strumento per la consultazione di dati geologici e di pericolosità sismica riferiti all'intero territorio nazionale. XIV Convegno di Ingegneria Sismica (ANIDIS), Bari 18-22 Settembre 2011. (in Italian).

Dolšek, M. (2010). Development of computing environment for the seismic performance assessment of reinforced concrete frames by using simplified nonlinear models. *Bulletin of Earthquake Engineering*, 8(6), 1309-1329.

Dolšek, M., Fajfar, P. (2004). Inelastic spectra for infilled reinforced concrete frames. Earthquake Engineering and Structural Dynamics, 33(15), 1395-1416.

Dolšek, M., Fajfar, P. (2005). Simplified non-linear seismic analysis of infilled reinforced concrete frames. Earthquake Engineering and Structural Dynamics, 34(1), 49-66.

Dolšek, M., Fajfar, P. (2008). The effect of masonry infills on the seismic response of a four-storey reinforced concrete frame – a deterministic assessment. Engineering Structures, 30(7), 1991-2001.

EPICentre Field Observation Report No. EPI-FO-200512 (2012), The 20th May 2012 EmiliaRomagna Earthquake, [available at http://www.ucl.ac.uk/~ucestor/research-earthquake/EPICentre_Report_EPI-FO-200512-v2.pdf].

EPICentre Field Observation Report No. EPI-FO-290512 (2012), The 29th May 2012 EmiliaRomagna Earthquake, [available at http://www.ucl.ac.uk/~ucestor/research-earthquake/EPICentre_Report_EPI-FO-290512.pdf].

Erberik M.A., 2008. Fragility-based assessment of typical mid-rise and low-rise RC buildings in Turkey. Engineering Structures, 30(5), 1360-1374.

Fiorini E., Borzi B., Iaccino R., 2012. Real Time damage scenario: case study for the L'Aquila earthquake. Proceedings of the 15th World Conference on Earthquake Engineering, September 24-28, Lisbon, Portugal. Paper 3707.

GNDT, 2000. Censimento di vulnerabilità a campione dell'edilizia corrente dei Centri abitati, nelle regioni Abruzzo, Basilicata, Calabria, Campania, Molise, Puglia e Sicilia. CNR-Gruppo Nazionale per la Difesa dai Terremoti, Rome, Italy.

Grünthal, G. ed. 1998. 'European Macroseismic Scale 1998 (EMS–98)', Cahiers du Centre Européen de Géodynamique et de Séismologie 15, Helfent-Betrange (Luxembourg).

Kappos A.J., Lekidis V., Panagopoulos G., Sous I., Theodulidis N., Karakostas Ch., Anastasiadis T., Salonikios T., Margaris B., 2007. Estimation of economic loss for buildings in the area struck by the 1999 Athens earthquake and comparison with actual repair costs. Earthquake Spectra, 23(2), 333-355.

Haselton, C.B., A.B. Liel, S. Taylor Lange, and G.G. Deierlein (2008). Beam-Column Element Model Calibrated for Predicting Flexural Response Leading to Global Collapse of RC Frame Buildings, PEER Report 2007/03, Pacific Engineering Research Center, University of California, Berkeley, California.

ISTAT, 2001. 14° censimento generale della popolazione e delle abitazioni (*14th general census of population and dwellings*). Istituto Nazionale di Statistica (*Italian National Instistute of Statistics*).

Iervolino I., De Luca F., Chioccarelli E. (2012) Engineering seismic demand in the 2012 Emilia sequence: preliminary analysis and model compatibility assessment. Annals of Geophysics, 55, 4: 639-645.

Liberatore L., Sorrentino L., Liberatore D., Decanini L.D. (2013). Performance of reinforced concrete residential buildings during the Emilia (Italy) 2012 Earthquakes. SE-50EEE International Conference on Earthquake Engineering, 29-31 May 2013, Skopje, Macedonia. Paper 409.

Lin L., Giovinazzi S., Pampanin S., 2012. Loss estimation in Christchurch CBD following recent earthquakes: validation and refinement of current procedures. Proceedings of the 2012 NZSEE Annual Conference, New Zealand Society for Earthquake Engineering, April 13-15, University of Canterbury, Christchurch, New Zealand. Paper 82.

Luco, N., Bazzurro,P. and Cornell,C.A. (2004). Dynamic versus static computation of the residual capacity of a mainshock-damaged building to withstand an aftershock. Proceedings of the 13th World Conference on Earthquake Engineering. 2004.

Manfredi G., Prota A., Verderame G.M., De Luca F., Ricci P., (2013). 2012 Emilia earthquake, Italy: Reinforced Concrete buildings response, Bulletin of Earthquake Engineering (under review).

McKay, M.D., Conover, W.J., Beckman, R.J. (1979). A comparison of three methods for selecting values of input

McKenna, F., Fenves, G.L., Scott, M.H. (2004). OpenSees: Open System for Earthquake Engineering Simulation. Pacific Earthquake Engineering Research Center. University of California, Berkeley, CA, USA. http://opensees.berkeley.edu.

Ordinanza del Presidente del Consiglio dei Ministri n. 3274 del 20/3/2003 (2003) Primi elementi in materia di criteri generali per la classificazione sismica del territorio nazionale e di normative tecniche per le costruzioni in zona sismica. G.U. n. 105 dell'8/5/2003 (in Italian).

Panagiotakos, T.B., Fardis, M.N. (1996). Seismic response of infilled RC frames structures. 11th WorldConference on Earthquake Engineering, Acapulco, México, June 23-28. Paper No. 225.

Panagiotakos, T.B. and Fardis, M.N. (2001). Deformations of Reinforced Concrete Members at Yielding and Ultimate, ACI Structural Journal, 98(2), 135-148.

Parisi F., De Luca F., Petruzzelli F., De Risi R., Chioccarelli E., Iervolino I. (2012) Field inspection after the May 20th and 29th 2012 Emilia-Romagna earthquakes, available at http://www.reluis.it..

Pinto, P.E., Giannini, R., Franchin, P. (2004). Seismic reliability analysis of structures. IUSS Press, Pavia, Italy.

Polese, M., Di Ludovico, M., Prota, A., & Manfredi, G. (2012). Damage-dependent vulnerability curves for existing buildings. Earthquake Engineering & Structural Dynamics.

Regio Decreto Legge n. 2229 del 16/11/1939. Norme per la esecuzione delle opere in conglomerate cementizio semplice od armato. G.U. n. 92 del 18/04/1940. (in Italian)

Ricci, P. (2010). Seismic vulnerability of existing RC buildings. Ph.D. Thesis. University of Naples Federico II, Naples, Italy.

Ricci, P., De Luca, F., Verderame, G.M. (2011). 6th April 2009 L'Aquila earthquake, Italy – Reinforced concrete building performance. Bulletin of Earthquake Engineering 9(1),285-305.

Ricci P., De Risi M.T., Verderame G.M., Manfredi G., (2013). Influence of infill distribution and design typology on seismic performance of low- and mid-rise RC buildings. Bulletin of Earthquake Engineering, DOI 10.1007/s10518-013-9453-4.

Rossetto T., Elnashai A. (2005). A new analytical procedure for the derivation of displacement-based vulnerability curves for populations of RC structures. Engineering Structures, 7(3), 397-409.

Shing, P. B. and Mehrabi A. B. (2002) "Behaviour and analysis of masonry-infilled frames", Progress in Structural Engineering and Materials; 4:320–331.

Spence R., Bommer J., Del Re D., Bird J., Aydinoğlu N., Tabuchi S., 2003. Comparing loss estimation with observed damage: a study of the 1999 Kocaeli earthquake in Turkey. Bulletin of Earthquake Engineering, 1(1), 83-113.

Stucchi M, Meletti C, Montaldo V, Crowley H, Calvi GM, Boschi E. (2011). Seismic Hazard Assessment (2003-2009) for the Italian Building Code, Bulletin of the Seismological Society of America 2011; 101(4):1885-1911.

Tertulliani A., Arcoraci L., Berardi M., Bernardini F., Camassi R., Castellano C., Del Mese S., Ercolani E., Graziani L., Leschiutta I., Rossi A., Vecchi M., 2011. An application of EMS98 in a medium-sized city: The case of L'Aquila (Central Italy) after the April 6, 2009 Mw 6.3 earthquake. Bulletin of Earthquake Engineering, 9(1), 67-80.

Verderame G.M., De Luca F., Ricci P., Manfredi G. (2011) Preliminary analysis of a soft-storey mechanism after the 2009 L'Aquila earthquake. Earthquake Engineering and Structural Dynamics, 40(8), pp. 925-944.

Verderame G.M., Polese M., Mariniello C., Manfredi G. (2010a). A simulated design procedure for the assessment of seismic capacity of existing reinforced concrete buildings, Advances in Engineering Software, 41, 323–335.

Verderame GM, Iervolino I, Ricci P (2009) Report on the damages on buildings following the seismic event of 6th of April 2009 time 1.32 (UTC)—L'Aquila M=5.8, V1.20, available at http://www.reluis.it/.

Verderame GM, Stella A., Cosenza E. (2001). Le proprietà meccaniche degli acciai impiegati nelle strutture in c.a. realizzate negli anni 60'. X Convegno nazionale "L'Ingegneria Sismica in Italia", Potenza-Matera, 9-13 September.

Verderame, G.M., Ricci, P., Manfredi, G., Cosenza, E. (2010b). Ultimate chord rotation of RC columns with smooth bars: some considerations about EC8 prescriptions. Bulletin of Earthquake Engineering, 8(6),1351-1373.

Verderame, G.M., Ricci, P., Esposito, M., Manfredi, G. (2012). STIL v1.0 – Software per la caratterizzazione delle proprietà meccaniche degli acciai da c.a. tra il 1950 e il 2000, available at http://www.reluis.it/.

Vidic T, Fajfar P, Fischinger M (1994) Consistent inelastic design spectra: strength and displacement. EarthqEng Struct Dyn 23(5):507–521

Vorechovsky, M., Novak, D. (2009). Correlation control in small-sample Monte Carlo type simulations I: A simulated annealing approach. Probabilistic Engineering Mechanics, 24(3), 452-462.